Electrochemistry Communications 104 (2019) 106483

Contents lists available at ScienceDirect

Electrochemistry Communications

journal homepage: www.elsevier.com/locate/elecom

Electrospun ceramic nanofibers as 1D solid electrolytes for lithium batteries

Andrea La Monaca[a,b], Andrea Paolella[a], Abdelbast Guerfi[a], Federico Rosei[b], Karim Zaghib[a,*]

[a] Centre d'excellence en électrification des transports et stockage d'énergie, Hydro-Québec, 1806 Boulevard Lionel-Boulet, Varennes, Québec J3X 1S1, Canada
[b] Centre Énergie, Matériaux et Télécommunications, Institut National de la Recherche Scientifique, 1650 Boulevard Lionel-Boulet, Varennes, Québec J3X 1S2, Canada

ARTICLE INFO

Keywords:
Electrospinning
Solid electrolyte
Ceramic
Nanofibers
Lithium metal battery

ABSTRACT

All-solid-state lithium batteries (ASSLBs) are undoubtedly among the most promising technologies to replace conventional lithium-ion batteries. Their key component is a thin solid-state electrolyte, which is safer than its flammable liquid counterpart and enables the use of metallic lithium, thus ensuring high energy densities (over 500 W h kg^{-1}). Several solid electrolytes are currently being investigated, such as NASICON-like materials, perovskites, and garnets. Typical techniques used to synthesize most such electrolytes still involve prolonged high-temperature calcination and sintering steps. An alternative approach is to couple electrospinning with the well-known sol–gel method to lower the temperatures and synthesis times and simultaneously exploit the benefits of using anisotropic nanostructured materials. In this review, we discuss advances in the synthesis of ceramic nanofibrous materials having high ionic conductivity and present our perspective regarding their potential application as electrolytes in ASSLBs.

1. Introduction

After the commercial deployment of the lithium-ion battery (LIB) by Sony Corp. in 1991 [1], the scientific community quickly realized the intrinsic safety limits of this technology, which mainly arise from the use of a flammable liquid electrolyte [2]. Therefore, in addition to the optimization of LIBs, the quest for a new, safer technology began. Currently the all-solid-state lithium battery (ASSLB) is widely considered as the best candidate to replace LIBs. The ASSLB is also based on the typical Li-ion "shuttle" mechanism but replaces the liquid electrolyte with a highly ion-conductive solid-state electrolyte (SSE) made of polymers [3,4], ceramics [5,6], or hybrid ceramic-polymers [7–9]. The main improvement associated with SSEs is increased device safety resulting from improved thermal and chemical stabilities and higher mechanical strength, which can physically hinder lithium dendritic growth. Another major advantage stems from the possibility of using metallic lithium as an anode, which can significantly improve the energy density of batteries because of the low redox potential (−3.04 V vs. SHE), high theoretical capacity (3860 mA h g^{-1}), and low density (0.59 g cm^{-3}). However, the solid nature of the electrolyte makes it difficult to establish optimal contact with the electrodes, thus increasing the interface resistance. Another challenge is related to the ionic conductivity of the SSE at room temperature, which ranges between 10^{-7} and 10^{-3} S cm^{-1}, and is typically lower than those of liquid counterparts, leading to weak performance at high C-rates. Among all the materials investigated to date, such as LISICON-like materials, NASICON-like materials, perovskites, garnets, sulfides, argyrodites, anti-perovskites, nitrides, and LiPON-type materials, only a few have ionic conductivity values comparable to those of liquid systems (~10^{-2} S cm^{-1}) [10,11]. To obtain efficient ionic transport, the material also needs to be as compact as possible. In addition, current synthesis methods and pelletizing processes usually require pressing treatments and high-temperature sintering, which increase the cost and limit the potential for mass production. In this context, numerous research efforts have focused on developing more convenient strategies to reduce the void spaces between SSE particles and improve the particle-to-particle contact, aiming to reduce the grain boundary resistance. Grain boundary resistance, which originates from the interface between crystallites in polycrystalline materials, greatly lowers the total ionic conductivity of SSEs thus limiting their potential application. To this end, the use of one-dimensional (1D) materials such as nanofibers and nanowires has recently been explored, as their morphology could be beneficial for achieving closer

Abbreviations: ASSLB, all-solid-state lithium battery; LIB, lithium-ion battery; SSE, solid-state electrolyte; SHE, standard hydrogen electrode; 1D, one-dimensional; 3D, three-dimensional; SEM, scanning electron microscopy; LLTO, $Li_{0.33}La_{0.557}TiO_3$; PVP, polyvinylpyrrolidone; DMF, dimethylformamide; AcOH, acetic acid; PAN, polyacrylonitrile; PEO, poly(ethylene oxide); LiTFSI, lithium bis(trifluoromethanesulfonyl)imide; LLZO, $Li_7La_3Zr_2O_{12}$; LATP, $Li_{1.3}Al_{0.3}Ti_{1.7}(PO_4)_3$; THF, tetrahydrofuran; PVdF-HFP, poly(vinylidene fluoride-co-hexafluoropropylene); iPrOH, isopropyl alcohol; EtOH, ethanol; acac, acetylacetone; RT, room temperature

* Corresponding author.
E-mail address: zaghib.karim@ireq.ca (K. Zaghib).

https://doi.org/10.1016/j.elecom.2019.106483
Received 17 May 2019; Received in revised form 17 June 2019; Accepted 18 June 2019
Available online 19 June 2019

packing and thus more effective densification during the sintering step. As suggested by Yang et al., connected crystallites inside nanowires are less susceptible to form agglomerates than nanoparticles, and this is beneficial for achieving higher densities. During sintering, agglomerates can reach near-full density while inter-agglomerates pores are very difficult to fill. This results from the surface energies of sintered agglomerates, which become too low to drive a further densification [12,13]. Hence, using nanowires instead of nanoparticles makes the sintering more effective, resulting in lower grain boundary resistances and thus higher ionic conductivities.

Spinning is a suite of manufacturing techniques used to fabricate fibers by using a polymer carrier. They require precursor materials to be in a fluid state to be spun, hence a facile approach used on large scale production is to melt them and then extrude them through a spinneret. This process is known as melt-spinning and was recently used by He et al. to grow $Li_{1.5}Al_{0.5}Ge_{1.5}(PO_4)_3$ glass-ceramic fibers [14]. Electrospinning is a widely used and versatile technique for fabricating nanofibers. It has been employed in many types of research, including the synthesis of energy materials. Unlike melt-spinning, electrospinning is conducted in solution rather than on a melt, so it does not require to liquefy the inorganic precursors. In addition, it is possible to finely control the diameter of electrospun fibers down to a few nanometers just by tuning the electric field, whereas the diameter of melt-spun fibers is limited by the spinneret dimensions. Several reviews have reported the development of electrospun materials for energy applications [15–18] and more specifically for anodes, cathodes, and separators for secondary batteries [19–22]. Examples of gel polymer electrolytes based on electrospun poly(vinylidene fluoride)-based scaffolds for improving the safety of LIBs have also been reported [23–27]. This hybrid approach was a first step toward increased safety, but the system remains flammable because organic solvents are still employed to produce the gel. More recently, electrospinning has been used to fabricate highly ion-conductive materials with fiber-like morphology [12,13,28-37]. Although they are used mainly as inorganic scaffolds to improve the performance of polymer electrolytes, some groups have proposed using ceramic nanowires as an SSE owing to the promising properties induced by their morphology. We speculate that such nanostructured 1D ceramics will be beneficial for the development of SSEs.

Our aim in this perspective is to analyze and compare highly ion-conductive materials that are prepared by electrospinning and thus are potentially relevant for future ASSLB applications. To this end, we discuss the synthesis and processing methods, resulting morphologies and overall properties. In addition, we also evaluate the potential advantages and main challenges to provide a realistic assessment of technological developments.

2. Electrospinning

2.1. History and fundamentals

The term “electrospinning” is a blend word from “electrostatic” and “spinning” and was introduced around 1993. However, the initial studies and patents on this technique date to the beginning of the 1900s. Among them, Formhals developed and patented an apparatus for producing artificial filaments [38]. A milestone for the development of electrospinning was the work conducted in 1969 by Taylor on the conical shape of electrically driven jets [39], later referred to by following researchers as “Taylor cone”. Only in the late 1900s and early 2000s an upsurge of research on electrospinning has been recorded, as a result of the growing interest in nanotechnology. Electrospinning thus became a simple and versatile technique to prepare polymeric fibers with high surface area and nano-sized diameter, breaking new grounds for future technologies and applications.

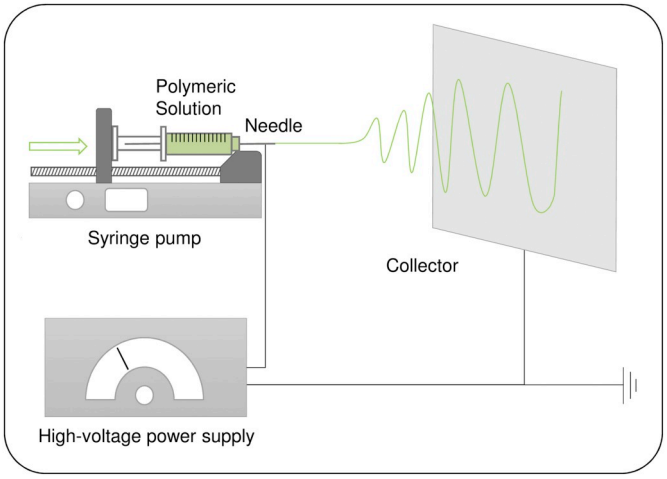

Fig. 1. Schematic of a typical electrospinning apparatus. The polymeric solution is spun onto a collector by means of the electric field generated by a high-voltage power supply.

2.2. Process

Electrospinning is a spinning technique used to prepare nanofibers from a polymeric solution by means of electrostatic forces. In a typical process the polymer is dissolved in a solvent system to form the polymeric solution. The solution is then spun using a typical apparatus as shown in Fig. 1. It is composed of a syringe connected to a syringe pump that controls the flow rate, a high-voltage power supply that induces electric charges on the syringe's needle, and a grounded or oppositely charged collector, which can be a plate or a rotating drum [40,41]. The polymeric solution is loaded into the syringe and flows inside the charged needle. A droplet forming on the tip of the needle is attracted toward the collector and is thus deformed into the so-called Taylor cone. The cone then becomes a jet, which is continuously stretched during an unstable and chaotic flight [42,43]. During this process, the solvent evaporates quickly, resulting in the deposition of dry, randomly distributed polymeric fibers on the collector. After a prolonged deposition period, a nonwoven mat is obtained.

2.3. Operational parameters

The fibers' dimensions and shape are influenced by several variables. Most of them can be categorized as solution parameters or process parameters [44]. The former are typical features of the polymeric solution, i.e., the concentration and molecular weight of the polymer, solution viscosity, and physicochemical properties of the solvent system. The latter type of parameters, such as the solution flow rate, applied voltage, and distance between the needle and collector, can be tuned during the electrospinning process. Typically, a balance among all the parameters has to be found to successfully deposit fibers with suitable shapes and the desired diameter [45]. Other variables can influence the electrospinning process, such as the temperature and relative humidity, the collector shape and motion, the needle inner diameter, and the angle between the needle and collector [43,44].

3. Electrospinning of ceramic nanofibers

To obtain ceramic nanofibers by electrospinning, a sol–gel step is necessary [46,47]. The sol–gel technique is based on the preparation of a homogeneous solution of cationic ingredients, which is gradually dried to obtain first a viscous sol and then a transparent amorphous solid known as a gel. The gel is finally annealed to crystallize the final product and simultaneously remove the remnant volatile components and organic side groups. To use sol–gel for electrospinning, a solution

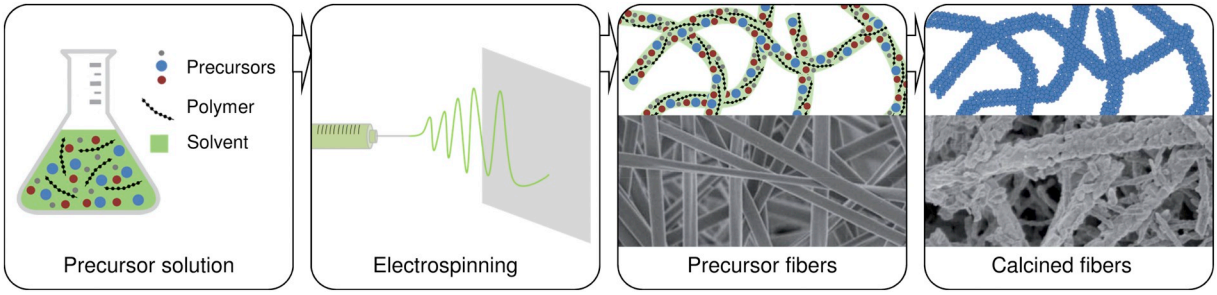

Fig. 2. Schematic of the preparation of ceramic fibers by electrospinning. The sol–gel precursor solution is electrospun to obtain precursor fibers. After calcination, ceramic fibers are obtained.
Scanning electron microscopy (SEM) images are adapted with permission from [31]. (Copyright 2018 Royal Society of Chemistry).

with both sol–gel precursors and a polymer carrier is prepared. All the components must be perfectly soluble in the selected solvent system to obtain a homogeneous distribution of the precursors and stable electrospinning. Therefore, after the solution parameters and the ratio between the polymer and precursor materials are optimized, the prepared solution is electrospun to obtain precursor nanofibers [48]. In the sol–gel synthesis, a high-temperature calcination step is finally performed to remove the polymer and all the organic side groups and crystallize the product. Owing to the void space within the fibrous network, product crystallization is confined within each fiber; thus, the final product retains the nanostructured morphology [48]. The typical steps are displayed in Fig. 2.

4. Ceramic nanofibers as electrolyte

The synthesis of ceramic nanofibers by electrospinning was initially reported in 2002 and 2003, describing fibers made of simple oxides such as titania [49,50], silica [50,51], and alumina-borate oxide [52]. Since then, highly ion-conductive materials have also been prepared using the same approach.

4.1. $Li_{0.33}La_{0.557}TiO_3$

A nanofibrous $Li_{0.33}La_{0.557}TiO_3$ (LLTO) solid electrolyte prepared by electrospinning was reported in 2005 [12,28]. LLTO, which was initially proposed as a solid electrolyte by Inaguma et al., crystallizes in the perovskite structure [53]. A high bulk conductivity of 1×10^{-3} S cm^{-1} was reported, but the total conductivity was lower, mainly because of high grain boundary resistance. Moreover, LLTO was observed to be electrochemically unstable below 1.8 V vs. Li^+/Li because of the reduction of Ti^{4+} [6]. Liu et al. investigated the properties of LLTO nanowires for use as a ceramic filler for polymer electrolytes [28]. As reported in Table 1, they used polyvinylpyrrolidone (PVP) as a polymer carrier and a binary solvent consisting of dimethylformamide (DMF) and acetic acid (AcOH). The as-spun fibers were calcined for 2 h at 600–900 °C. The diameter of the calcined fibers then decreased from 220 to 140 nm by increasing the temperature from 700 to 800 °C. By contrast, at 900 °C an average diameter of 150 nm was reported, together with coarse surfaces resulting from grain growth. A 15 wt% nanowire content improved the ionic conductivity of a polyacrylonitrile-lithium perchlorate (PAN-$LiClO_4$) electrolyte by approximately three orders of magnitude, whereas an LLTO-nanoparticle-filled PAN-$LiClO_4$ electrolyte exhibited an improvement of only one order of magnitude. In contrast to the case of nanoparticles, ceramic nanofibers created a 3D ion-conducting pathway, which improved the long-range Li^+ transport (Fig. 3). According to Wieczorek et al. [54], the ionic conductivity enhancement may be partly attributed to the strong affinity between ClO_4^- and acidic groups on the surface of nano-oxides, which facilitates the $LiClO_4^-$ dissociation and increases the concentration of Li^+. Moreover, Liu et al. proposed that the high number of vacancies on the LLTO surface is beneficial for Li^+ hopping mechanism, thus further improving its ionic transport [28]. In the same year, Yang et al. reported the potential application of LLTO nanowires as an SSE for lithium batteries [12]. They synthesized them by electrospinning a water-based sol and performing a calcination step for 3 h at 1000 °C. The resulting polycrystalline fibers, which consisted of the pure tetragonal phase, had diameters of 100–200 nm. Yang et al. successfully prepared pellets from LLTO nanowires; they reported higher density and improved ionic conductivity compared to those of pellets made of LLTO particles synthesized by a conventional sol–gel route. Cross-sectional images are shown in Fig. 3b. Interesting results on LLTO nanofibers were reported by Liu et al. [29], who investigated the effect of fiber alignment on the ionic conductivity of composite polymer electrolytes using interdigitated Pt electrodes (Fig. 3a). They synthesized the LLTO nanofibers by spinning the precursor solution directly onto the Pt electrode and then calcined the fibers for 2 h at 800 °C. They showed that when well-aligned perpendicularly oriented nanowires were used, the conductivity was one order of magnitude larger than

Table 1
Synthesis parameters and fiber properties of SSEs obtained by electrospinning.

SSE formula	Polymer carrier	Solvent system[1]	Calcination conditions	Fiber diameter	Electrolyte composition	Ionic conductivity[2] (S cm^{-1})	Ref.
$Li_{0.33}La_{0.557}TiO_3$	PVP	H_2O/iPrOH/AcOH	1000 °C (3 h)	100–200 nm	LLTO pellet	4.37×10^{-6} (RT)	[12]
	PVP	DMF/AcOH	600–900 °C (2 h)	140–220 nm	PAN-$LiClO_4$ + 15 wt% LLTO	2.4×10^{-4} (RT)	[28]
	PVP	DMF/AcOH	800 °C (2 h)	138 nm	PAN-$LiClO_4$ + 3 wt% LLTO	6.05×10^{-5} (30 °C)	[29]
	PVP	DMF/AcOH	800 °C (2 h)	1 μm	PEO-LiTFSI + 5 wt% LLTO	5.53×10^{-5} (25 °C)	[30]
	PVP	DMF/AcOH	700–900 °C (2 h)	110–374 nm	PEO-LiTFSI + 15 wt% LLTO	2.4×10^{-4} (25 °C)	[31]
$Li_7La_3Zr_2O_{12}$	PVP	H_2O/iPrOH/AcOH	700 °C (2.5 h)	–	–	–	[13]
	PVP	DMF/AcOH	800 °C (2 h)	138 nm	PEO-LiTFSI + LLZO mat	2.5×10^{-4} (RT)	[32]
	PVP	DMF/iPrOH/AcOH	700 °C (1 − 3*h*)	100–276 nm	PAN-$LiClO_4$ + 5 wt% LLZO	1.31×10^{-4} (20 °C)	[33]
	PVP	DMF	700 °C (2 h)	100–200 nm	PEO-LiTFSI + 10 wt% LLZO	2.39×10^{-4} (25 °C)	[34]
$Li_6Zr_2O_7$	PVP	H_2O/EtOH	750 °C (1 h)	100 nm	Fibers	1.27×10^{-5} (200 °C)	[35]
$Li_{1.3}Al_{0.3}Ti_{1.7}(PO_4)_3$	PVdF-HFP	DMF/THF/acac	800–950 °C (2 h)	270 nm	Porous mat	3×10^{-7} (RT)	[36]

[1] H_2O: deionized water; iPrOH: isopropyl alcohol; EtOH: ethanol; acac: acetylacetone.
[2] Ionic conductivity values resulted from the corresponding electrolyte compositions.

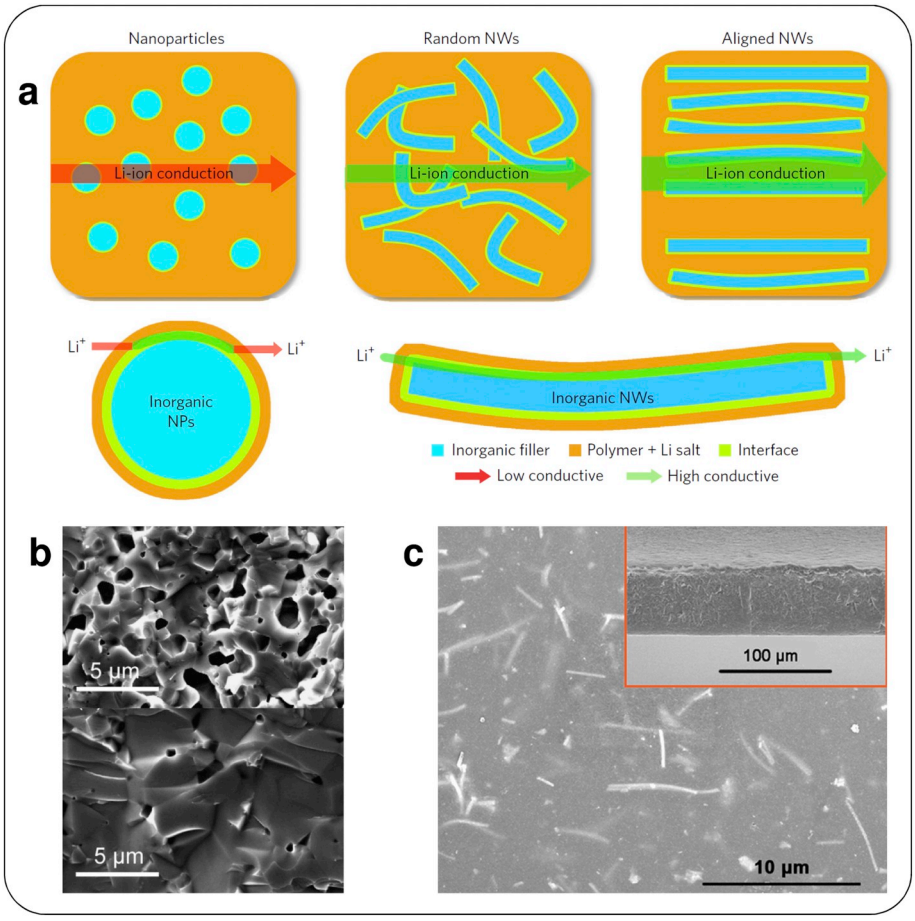

Fig. 3. (a) Possible Li-ion conduction pathways in composite polymer electrolyte (adapted with permission from [29]; copyright 2017 Springer Nature); (b) cross-sectional SEM image of pellet made of conventional sol–gel LLTO (top) and LLTO nanofibers (bottom) (adapted with permission from [13]; copyright 2015 Elsevier); (c) morphology of composite polymer electrolyte with 15 wt% nanowire filler (Adapted with permission from [28]; copyright 2015 American Chemical Society).

that of randomly oriented nanowires. The calculated surface conductivity of the nanowires was on the order of 10^{-2} S cm^{-1} at 30 °C, which is close to the typical values for liquid systems, indicating that the improved conductivity results from the absence of crossing junctions in the aligned sample. Moreover, they confirmed the previously proposed effect of LLTO surface vacancies on Li^+ transport [28]. They observed a smaller ionic conductivity enhancement when using inert ceramic fillers (ZrO_2 nanowires) instead of LLTO nanowires, thus showing the benefits of using highly ion-conductive fillers [29]. Recently, two more papers on the use of LLTO nanowires as a ceramic filler for poly(ethylene oxide)-lithium bis(trifluoromethanesulfonyl) imide (PEO-LiTFSI) electrolytes [30,31] reported improvements in the ionic conductivity and electrochemical stability.

4.2. $Li_7La_3Zr_2O_{12}$

Since its discovery in 2007 [55], the cubic garnet $Li_7La_3Zr_2O_{12}$ (LLZO) has attracted great interest owing to its good electrochemical stability and an ionic conductivity of 3×10^{-4} S cm^{-1} at 25 °C, with a relatively low grain boundary resistance [6]. Few studies on the preparation of LLZO nanowires by electrospinning have been reported to date [13,32–34]. A water-based sol was electrospun using either nitrate or acetate precursor salts and PVP; then, after electrospinning, the effect of calcination time on the morphology and structure of the LLZO fibers was investigated. The optimal time was found to be 2.5 h; at shorter times, the main phase was still $La_2Zr_2O_7$, whereas the fibers started to coalesce to form larger ligament-like structures after 3 h (Fig. 4a) [13]. However, it takes at least 3 h to produce a pure cubic LLZO phase. Later studies reported the electrospinning of a DMF-based sol with nitrate precursors and PVP as a polymer carrier [32,33]. Unlike the previous work, the pure cubic LLZO phase was obtained after only

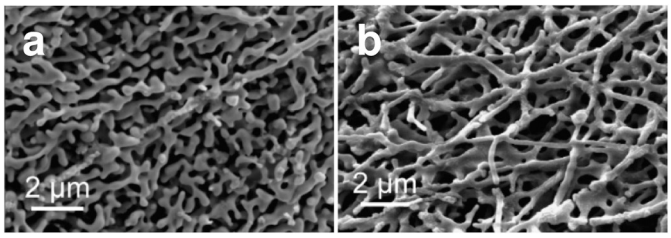

Fig. 4. SEM images of electrospun LLZO calcined at 700 °C. (a) Ligament-like structure obtained by using aqueous precursors after a 3 h calcination step; (b) nanofibers prepared using DMF-based precursors and calcined for 1 h. (Adapted with permission from [33]; copyright 2017 American Chemical Society).

1–2 h of calcination. Moreover, despite the short calcination time, a good fiber morphology was maintained, and no coalescence into the ligament-like structure was observed (Fig. 4b). Fu et al. then poured a solution of PEO-LiTFSI onto the ceramic mat to achieve a hybrid ceramic-polymer electrolyte with enhanced mechanical properties and fast lithium ion conduction. In addition they demonstrated effective suppression of lithium dendrite growth by successfully cycling Li symmetric cells for 1000 h [32]. Yang et al. added various quantities of LLZO nanowires to a PAN-$LiClO_4$ electrolyte, and the highest ionic conductivity was obtained when 5 wt% of the filler was used; this value is approximately three orders of magnitude higher than that of plain PAN-$LiClO_4$ [33]. Al- and Ta-doped LLZO were also synthesized and investigated, yet the ionic conductivity of the corresponding composite polymer electrolytes was similar to that of electrolytes prepared with undoped LLZO. A recent study of LLZO nanowires as a ceramic filler for a PEO-LiTFSI electrolyte was reported by Wan et al. [34]. The resulting

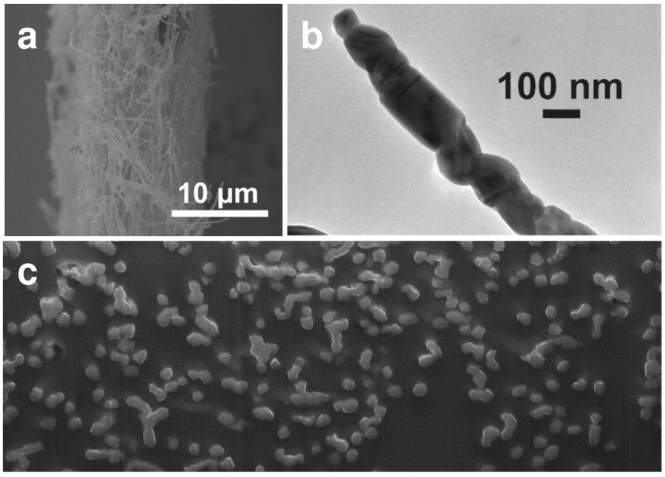

Fig. 5. (a) Cross-sectional SEM image of self-standing LATP membrane after electrospinning and calcination. (b) Transmission electron microscopy images of isolated fibers (c) Cross-sectional field emission gun SEM image of a hybrid LATP/PVdF-HFP membrane.
(Adapted with permission from [36]; copyright 2017 American Chemical Society).

hybrid electrolyte was characterized by a better ionic conductivity and an effective suppression of lithium dendrite growth.

4.3. Others

Lithium zirconate is a class of materials studied mainly for energy and environmental applications owing to their good ionic conductivity and high lithium content. Precursor salts and PVP were dissolved in a binary solvent of water and ethanol (4:6 mass ratio), which was then electrospun to obtain $Li_6Zr_2O_7$ nanofibers [35]. Pure-phase $Li_6Zr_2O_7$ nanofibers were obtained after the precursor fibers were calcined for 1 h at 750 °C. The authors of this study reported a negligible grain boundary resistance; thus, they speculated that the ionic conductivity of the nanofibers will be higher than that of the bulk material.

Another interesting work on the synthesis of a nanofibrous material with high ionic conductivity is that of Lancel et al. [36]. They reported the synthesis of $Li_{1.3}Al_{0.3}Ti_{1.7}(PO_4)_3$ (LATP) nanofibers to fabricate a composite membrane for lithium air batteries. LATP is the most intensively studied NASICON material owing to its high ionic conductivity (7×10^{-4} S cm^{-1} at 25 °C) and low cost [56]. The main drawback of LATP is the same as that of LLTO: easy reduction of Ti^{4+} below 2.5 V vs. Li^+/Li [6]. Here a DMF/tetrahydrofuran (THF) binary solvent was used to dissolve the precursors and polymer carrier. As in the other cases, PVP has been investigated as a polymer carrier, but when it was used, the microstructure of the electrospun fibers was too dense, resulting in coalescence and morphology loss after calcination [57]. Hence, poly(vinylidene fluoride-co-hexafluoropropylene) (PVdF-HFP) was used as the polymer carrier, and the electrospun fibers were then calcined for 2 h at 800–950 °C to obtain a pure LATP phase. The ionic conductivity of the resulting nanofibrous mat was 3×10^{-7} S cm^{-1}, which is lower than that of the bulk material. This is because of the mat porosity, which was estimated to be close to 60%. The mat was then impregnated with a solution of PVdF-HFP to obtain a watertight membrane for use as a separator in aqueous lithium air batteries (Fig. 5).

5. Conclusions and outlook

Electrospinning is probably the simplest technique to obtain nanometric elongated 1D structures such as nanowires and nanofibers, which exhibit promising properties. Some of these structures could be interesting for SSE applications, although this possibility has not yet been investigated extensively. To date, electrospinning has been used mainly to produce ceramic fillers for solid polymer electrolytes, which slightly improved their performance but without overcoming their limitations. Only Yang et al. [12] proposed using ceramic nanofibers as a pure solid electrolyte for ASSLBs. By demonstrating the more efficient densification and higher ionic conductivity of the fiber-based pellets, they proved the potential for integration of electrospinning into the preparation of future SSEs. The specific morphology of ceramic nanostructures can be beneficial for material synthesis and pellet production. As emphasized in the reviewed works, compared to conventional sol–gel routes, electrospinning can lower the calcination time and temperature [13,33], promote the formation of a specific phase [12,33], and help control the crystallite dimensions owing to confinement of crystallization within fibers [37]. Although electrospinning is a facile and low-cost technique for laboratory research, the low production rate, the potentially unsafe applied voltages and the high dependence on environmental conditions could limit a future industrial upscaling. However we speculate that, by employing 1D ceramic materials to develop SSEs, a higher mechanical strength can be obtained, thus enabling the development of thinner self-standing structures. Furthermore, thanks to continuous ionic transport pathways provided by the elongated morphology, the ionic conductivity can be increased, thus resulting in enhanced battery performance, especially at high C-rates. On these grounds, such 1D structures could be potentially crucial to the development of ASSLBs with better overall performance.

Acknowledgements

The project was supported by Hydro-Québec and by NSERC through a Collaborative Research and Development Grant. F.R. acknowledges partial salary support from the Canada Research Chairs program.

Declaration of Competing Interest

The authors declare no conflict of interest.

References

[1] T. Nagaura, K. Tozawa, Prog. Batter. Sol. Cells 9 (1990) 209.
[2] A. Mauger, C.M. Julien, A. Paolella, M. Armand, K. Zaghib, Mater. Sci. Eng. R 134 (2018) 1–21, https://doi.org/10.1016/j.mser.2018.07.001.
[3] Q. Zhang, K. Liu, F. Ding, X. Liu, Nano Res. 10 (2017) 4139–4174, https://doi.org/10.1007/s12274-017-1763-4.
[4] L. Long, S. Wang, M. Xiao, Y. Meng, J. Mater. Chem. A 4 (2016) 10038–10069, https://doi.org/10.1039/C6TA02621D.
[5] J.C. Bachman, S. Muy, A. Grimaud, H.-H. Chang, N. Pour, S.F. Lux, O. Paschos, F. Maglia, S. Lupart, P. Lamp, L. Giordano, Y. Shao-Horn, Chem. Rev. 116 (2016) 140–162, https://doi.org/10.1021/acs.chemrev.5b00563.
[6] F. Zheng, M. Kotobuki, S. Song, M.O. Lai, L. Lu, J. Power Sources 389 (2018) 198–213, https://doi.org/10.1016/j.jpowsour.2018.04.022.
[7] S. Zekoll, C. Marriner-Edwards, A.K.O. Hekselman, J. Kasemchainan, C. Kuss, D.E.J. Armstrong, D. Cai, R.J. Wallace, F.H. Richter, J.H.J. Thijssen, P.G. Bruce, Energy Environ. Sci. 11 (2018) 185–201, https://doi.org/10.1039/C7EE02723K.
[8] W. Zhang, J. Nie, F. Li, Z.L. Wang, C. Sun, Nano Energy 45 (2018) 413–419, https://doi.org/10.1016/j.nanoen.2018.01.028.
[9] L. Chen, Y. Li, S.-P. Li, L.-Z. Fan, C.-W. Nan, J.B. Goodenough, Nano Energy 46 (2018) 176–184, https://doi.org/10.1016/j.nanoen.2017.12.037.
[10] N. Kamaya, K. Homma, Y. Yamakawa, M. Hirayama, R. Kanno, M. Yonemura, T. Kamiyama, T. Kato, S. Hama, K. Kawamoto, A. Mitsui, Nat. Mater. 10 (2011) 682–686, https://doi.org/10.1038/nmat3066.
[11] Y. Seino, T. Ota, K. Takada, A. Hayashi, M. Tatsumisago, Energy Environ. Sci. 7 (2014) 627–631, https://doi.org/10.1039/C3EE41655K.
[12] T. Yang, Z.D. Gordon, Y. Li, C.K. Chan, J. Phys. Chem. C 119 (2015) 14947–14953, https://doi.org/10.1021/acs.jpcc.5b03589.
[13] T. Yang, Y. Li, C.K. Chan, J. Power Sources 287 (2015) 164–169, https://doi.org/10.1016/j.jpowsour.2015.04.044.
[14] K. He, P. Xie, C. Zu, Y. Wang, B. Li, B. Han, M.Z. Rong, M.Q. Zhang, RSC Adv. 9 (2019) 4157–4161, https://doi.org/10.1039/C8RA08401G.
[15] Q. Liu, J. Zhu, L. Zhang, Y. Qiu, Renew. Sust. Energ. Rev. 81 (2018) 1825–1858, https://doi.org/10.1016/j.rser.2017.05.281.
[16] G. Sun, L. Sun, H. Xie, J. Liu, Nanomaterials 6 (2016) 129, https://doi.org/10.3390/nano6070129.
[17] X. Shi, W. Zhou, D. Ma, Q. Ma, D. Bridges, Y. Ma, A. Hu, J. Nanomater. (2015)

140716, https://doi.org/10.1155/2015/140716.
[18] S. Cavaliere, S. Subianto, I. Savych, D.J. Jones, J. Rozière, Energy Environ. Sci. 4 (2011) 4761–4785, https://doi.org/10.1039/C1EE02201F.
[19] H.-G. Wang, S. Yuan, D.-L. Ma, X.-B. Zhang, J.-M. Yan, Energy Environ. Sci. 8 (2015) 1660–1681, https://doi.org/10.1039/C4EE03912B.
[20] J.-W. Jung, C.-L. Lee, S. Yu, I.-D. Kim, J. Mater. Chem. A 4 (2016) 703–750, https://doi.org/10.1039/C5TA06844D.
[21] E.S. Pampal, E. Stojanovska, B. Simon, A. Kilic, J. Power Sources 300 (2015) 199–215, https://doi.org/10.1016/j.jpowsour.2015.09.059.
[22] X. Zhang, L. Ji, O. Toprakci, Y. Liang, M. Alcoutlabi, Polym. Rev. 51 (2011) 239–264, https://doi.org/10.1080/15583724.2011.593390.
[23] X. Huang, S. Zeng, J. Liu, T. He, L. Sun, D. Xu, X. Yu, Y. Luo, W. Zhou, J. Wu, Phys. Chem. C 119 (2015) 27882–27891, https://doi.org/10.1021/acs.jpcc.5b09130.
[24] S.W. Choi, S.M. Jo, W.S. Lee, Y.R. Kim, Adv. Mater. 15 (2003) 2027–2032, https://doi.org/10.1002/adma.200304617.
[25] W. Li, Y. Wu, J. Wang, D. Huang, L. Chen, G. Yang, Eur. Polym. J. 67 (2015) 365–372, https://doi.org/10.1016/j.eurpolymj.2015.04.014.
[26] L. Zhou, Q. Cao, B. Jing, X. Wang, X. Tang, N. Wu, J. Power Sources 263 (2014) 118–124, https://doi.org/10.1016/j.jpowsour.2014.03.140.
[27] A. La Monaca, F. De Giorgio, M.L. Focarete, D. Fabiani, M. Zaccaria, C. Arbizzani, J. Electrochem. Soc. 164 (2017) A6431–A6439, https://doi.org/10.1149/2.0651701jes.
[28] W. Liu, N. Liu, J. Sun, P.-C. Hsu, Y. Li, H.-W. Lee, Y. Cui, Nano Lett. 15 (2015) 2740–2745, https://doi.org/10.1021/acs.nanolett.5b00600.
[29] W. Liu, S.W. Lee, D. Lin, F. Shi, S. Wang, A.D. Sendek, Y. Cui, Nat. Energy 2 (2017) 17035, , https://doi.org/10.1038/nenergy.2017.35.
[30] L. Zhu, P. Zhu, Q. Fang, M. Jing, X. Shen, L. Yang, Electrochim. Acta 292 (2018) 718–726, https://doi.org/10.1016/j.electacta.2018.10.005.
[31] P. Zhu, C. Yan, M. Dirican, J. Zhu, J. Zang, R.K. Selvan, C.-C. Chung, H. Jia, Y. Li, Y. Kiyak, N. Wu, X. Zhang, J. Mater. Chem. A 6 (2018) 4279–4285, https://doi.org/10.1039/C7TA10517G.
[32] K. Fu, Y. Gong, J. Dai, A. Gong, X. Han, Y. Yao, C. Wang, Y. Wang, Y. Chen, C. Yan, Y. Li, E.D. Wachsman, L. Hu, Proc. Natl. Acad. Sci. U. S. A. 113 (2016) 7094–7099, https://doi.org/10.1073/pnas.1600422113.
[33] T. Yang, J. Zheng, Q. Cheng, Y.-Y. Hu, C.K. Chan, ACS Appl. Mater. Interfaces 9 (2017) 21773–21780, https://doi.org/10.1021/acsami.7b03806.
[34] Z. Wan, D. Lei, W. Yang, C. Liu, K. Shi, X. Hao, L. Shen, W. Lv, B. Li, Q.-H. Yang, F. Kang, Y.-B. He, Adv. Funct. Mater. 29 (2019) 1805301, , https://doi.org/10.1002/adfm.201805301.
[35] Y. Liu, X. Hua, Int. J. Appl. Ceram. Technol. 13 (2016) 579–583, https://doi.org/10.1111/ijac.12529.
[36] G. Lancel, P. Stevens, G. Toussaint, M. Maréchal, N. Krins, D. Bregiroux, C. Laberty-Robert, Langmuir 33 (2017) 9288–9297, https://doi.org/10.1021/acs.langmuir.7b00675.
[37] C.K. Chan, T. Yang, J.M. Weller, Electrochim. Acta 253 (2017) 268–280, https://doi.org/10.1016/j.electacta.2017.08.130.
[38] A. Formhals, US Patent 1975504, 1934.
[39] G.I. Taylor, Proc. R. Soc. Lond. A 313 (1969) 453, https://doi.org/10.1098/rspa.1969.0205.
[40] T.J. Sill, H.A. von Recum, Biomaterials 29 (2008) 1989–2006, https://doi.org/10.1016/j.biomaterials.2008.01.011.
[41] D. Liang, B.S. Hsiao, B. Chu, Adv. Drug Deliv. Rev. 59 (2007) 1392–1412, https://doi.org/10.1016/j.addr.2007.04.021.
[42] T. Subbiah, G.S. Bhat, R.W. Tock, S. Parameswaran, S.S. Ramkumar, J. Appl. Polym. Sci. 96 (2005) 557–569, https://doi.org/10.1002/app.21481.
[43] W.E. Teo, S. Ramakrishna, Nanotechnology 17 (2006) R89–R106, https://doi.org/10.1088/0957-4484/17/14/R01.
[44] N. Bhardwaj, S.C. Kundu, Biotechnol. Adv. 28 (2010) 325–347, https://doi.org/10.1016/j.biotechadv.2010.01.004.
[45] Z.-M. Huang, Y.-Z. Zhang, M. Kotaki, S. Ramakrishna, Compos. Sci. Technol. 63 (2003) 2223–2253, https://doi.org/10.1016/S0266-3538(03)00178-7.
[46] R. Ramaseshan, S. Sundarrajan, R. Jose, J. Appl. Phys. 102 (2007) 111101, , https://doi.org/10.1063/1.2815499.
[47] H. Wu, W. Pan, D. Lin, H. Li, J. Adv. Ceram. 1 (2012) 2–23, https://doi.org/10.1007/s40145-012-0002-4.
[48] D. Li, J.T. McCann, Y. Xia, J. Am. Ceram. Soc. 89 (2006) 1861–1869, https://doi.org/10.1111/j.1551-2916.2006.00989.x.
[49] D. Li, Y. Xia, Nano Lett. 3 (2003) 555–560, https://doi.org/10.1021/nl034039o.
[50] B. Ding, H. Kim, C. Kim, M. Khil, S. Park, Nanotechnology 14 (2003) 532–537, https://doi.org/10.1088/0957-4484/14/5/309.
[51] C. Shao, H. Kim, J. Gong, D. Lee, Nanotechnology 13 (2002) 635–637, https://doi.org/10.1088/0957-4484/13/5/319.
[52] H. Dai, J. Gong, H. Kim, D. Lee, Nanotechnology 13 (2002) 674–677, https://doi.org/10.1088/0957-4484/13/5/327.
[53] Y. Inaguma, C. Liquan, M. Itoh, T. Nakamura, T. Uchida, H. Ikuta, M. Wakihara, Solid State Commun. 86 (93) (1993) 689–693 https://doi.org/10.1016/0038-1098.
[54] W. Wieczorek, Z. Florjanczyk, J.R. Stevens, Electrochim. Acta 40 (1995) 2251–2258, https://doi.org/10.1016/0013-4686(95)00172-B.
[55] R. Murugan, V. Thangadurai, W. Weppner, Angew. Chem. Int. Ed. 46 (2007) 7778–7781, https://doi.org/10.1002/anie.200701144.
[56] H. Aono, N. Imanaka, G.-Y. Adachi, Acc. Chem. Res. 27 (1994) 265–270, https://doi.org/10.1021/ar00045a002.
[57] . G. Lancel, Ph.D. thesis, Université Pierre et Marie Curie, Paris, 16th February 2016.